ELSEVIER

Catalysis Today 57 (2000) 71–86

CATALYSIS TODAY

www.elsevier.com/locate/cattod

Oxygenation of alkanes and aromatics by reductively activated oxygen during H_2–O_2 cell reactions

Kiyoshi Otsuka *, Ichiro Yamanaka

Department of Applied Chemistry, Graduate School of Science and Engineering, Tokyo Institute of Technology, Ookayama, Meguro-ku, Tokyo 152-8552, Japan

Abstract

Direct oxygenation of aromatics to phenols, C6 alkanes and light alkanes to alcohols and aldehydes are realized at the cathode during H_2–O_2 fuel cell reactions at room temperature. The advantages of these H_2–O_2 fuel cell systems compared with the common catalytic oxidation systems are demonstrated and the electrocatalysis of the cathodes and the reaction mechanisms for the oxygenations are discussed in detail. The topics are the ω-oxidation of *n*-hexane with ($FeCl_3$ + α-cyclodextrin)/graphite cathode, the synergism of Pd-black and iron compounds for the formation of phenol on (Pd-black + Fe_3O_4)/carbon-whisker (CW) cathode, cogeneration of phenol and electricity by using $CuSO_4$/CW cathode, the synergism of different carbon materials in the cathode for the product selectivity in the oxidation of toluene on (CW + Active Carbon) cathodes, and the oxidation of propane over (Pd-black + $VO(acac)_2$)/carbon-fiber cathodes in the gas phase. Reductive activation of oxygen on the cathode is essential for these oxygenations. For most of the electrocatalytic systems used in this work, the oxygenations of alkanes and aromatics can be explained on the basis of Fenton Chemistry assuming $HO^{\bullet}$ as the active oxygen species, except for the $SmCl_3$/graphite cathode.

Keywords: Benzene; Phenol; Light alkanes; H_2–O_2-fuel cell; Partial oxidation; Reductive activation of oxygen

1. Introduction

In the current chemical industry, syntheses of phenols from aromatics, alcohols from light alkanes and epoxides from alkenes (≥C3) are operated through multi-step processes. For example, phenol is manufactured by the Cumene Process via the production of cumene-hydroperoxide by auto-oxidation of cumene, methanol is synthesized from CH_4 via the synthesis gas, CO and H_2, produced by the steam reforming of CH_4, and propene oxide from propene and ethylbenzene-hydroperoxide prepared by the auto-oxidation of ethylbenzene. Thus, direct hydroxylation of aromatics to phenols with O_2, direct oxidation of lower alkanes (CH_4, C_2H_6, and C_3H_8) to alcohols, and epoxidation of propene to propene oxide are expected to be realized in the next century. However, these direct oxidations by conventional catalytic methods with O_2 are very difficult and still far from realization. Under these circumstances, it is suggested that one of the ideas to perform these direct oxidations with O_2 is to apply the reductive activation of O_2, as described below.

Typical examples of the reductive activation of O_2 can be seen in monooxygenase systems (cytochrome P-450 [1–4], methane monooxygenase [5,6], etc.). In the case of cytochrome P-450, it is generally believed that the O_2 adsorbed on the iron site (Fe^{III})

* Corresponding author. Tel.: +81-3-5734-2143; fax: +81-3-5734-2879.
E-mail address: kotsuka@o.cc.titech.ac.jp (K. Otsuka).

0920-5861/00/$ – see front matter
PII: S0920-5861(99)00310-7

of Fe–porphyrin is activated through the reduction with an electron donor such as NADH assisted by the electron-transfer system in the structure of the P-450. The reductive activation of O_2 and the subsequent oxygenation of hydrocarbons (R–H) can be expressed as a whole as follows:

$$O_2 + \text{Por–Fe}^{III} + \text{NADH} + H^+ \rightarrow \text{Por}^+\text{–Fe}^{IV}\text{=O} + H_2O + \text{NAD}^+ \quad (1)$$

$$\text{Por}^{+\bullet}\text{–Fe}^{IV}\text{=O} + \text{R–H} \rightarrow \text{R–OH} + \text{Por–Fe}^{III} \quad (2)$$

where the active oxygen species is an oxo species on high-valent iron on porphyrin cation radical ($\text{Por}^{+\bullet}\text{–Fe}^{IV}$=O). The similar reductive activation of O_2 on di-nuclear iron sites and the oxygenation of CH_4 to methanol are suggested for methane monooxygenase [5,6].

Many catalytic systems for the reductive activation of O_2 with various reducing agents ($NaBH_4$, ascorbic acid, Zn, aldehyde, phosphine, H_2, etc.) have been reported [1–4,7–10]. Among many reducing agents, the cheapest and handy reductant is H_2. Recently, several catalytic systems for oxygenation of hydrocarbons with a gas-mixture of O_2 and H_2 have been reported [10–16]. The catalysts (Cat) in these systems activate O_2 with H_2, producing active oxygen species (O*) which oxygenate hydrocarbons as follows:

$$O_2 + H_2 + \text{Cat} \rightarrow O^*(\text{Cat}) + H_2O \quad (3)$$

$$\text{R–H} + O^*(\text{Cat}) \rightarrow \text{R–OH} + \text{Cat} \quad (4)$$

Our new idea in this report is to activate O_2 by electrochemical reduction at the cathode during H_2–O_2 cell reactions, which enables the direct oxygenation of various hydrocarbons. In the case of a H_2–O_2 fuel cell using an acidic electrolyte, the electrochemical oxidation of H_2 to H^+ and e^- occurs at the anode (Eq. (5)) and the reduction of O_2 with H^+ and e^- to H_2O takes place at the cathode (Eq. (6)). The net reaction is the formation of water from H_2 and O_2.

$$\text{Anode}: \quad H_2 \rightarrow 2H^+ + 2e^- \quad (5)$$

$$\text{Cathode}: \quad \tfrac{1}{2}O_2 + 2H^+ + 2e^- \rightarrow H_2O \quad (6)$$

Here, if we choose a special electrocatalyst in the cathode, the electrochemical reduction of O_2 on the electrocatalyst is expected to generate an intermediate oxygen species, such as $^{\bullet}O^{\bullet}$ and $HO^{\bullet}$, which could be active for the oxygenation of hydrocarbons.

The oxygenation of hydrocarbons applying the H_2–O_2 fuel cell system described above has several advantages [13,17–21]: (i) The oxidation rate can be controlled easily by controlling the current with a variable resistor in the outer circuit. If it is needed, the oxidation of hydrocarbons can be immediately stopped by opening the circuit. (ii) When the product selectivities depend on the cathode potential, the optima conditions for the selectivities can be easily adjusted by controlling the potential. (iii) Since H_2 and O_2 are separated by a diaphragm holding electrolyte, the danger of explosion can be reduced compared with the catalytic systems using a mixture of H_2, O_2 and hydrocarbons [10–12,15,16].

With regard to the oxygenation by this H_2–O_2 fuel cell system, we describe the following three topics in this short review. The first topic is for the direct partial oxidation of alkanes and aromatics under mild conditions. The second topic is for the control of the product distributions by choosing a proper catalytic component in the cathode. Finally, the active oxygen species and the reaction mechanism for the cathodic oxygenation will be discussed.

2. Results and discussion

2.1. Partial oxidation of alkanes

2.1.1. Oxidation of cyclohexane during H_2–O_2 cell reactions

The H_2–O_2 fuel cell system for the oxidation of hydrocarbons was designed as indicated in Fig. 1. The system was composed of [O_2 (g), hydrocarbon (liq.), cathode | H_3PO_4 aq. (1 M) in silica–wool disk | (Pt-black mixed with graphite)-anode, H_2 (g)]. The silica–wool disk impregnated with H_3PO_4 aq. was used as an electrolyte membrane. The aqueous solution and hydrophobic hydrocarbon solution do not mix each other. Since, the electrochemical reduction of O_2 is believed to proceed at the three-phase boundary (hydrophilic phase of H_3PO_4 aq., hydrophobic phase of hydrocarbon, and solid phase of electrode) in

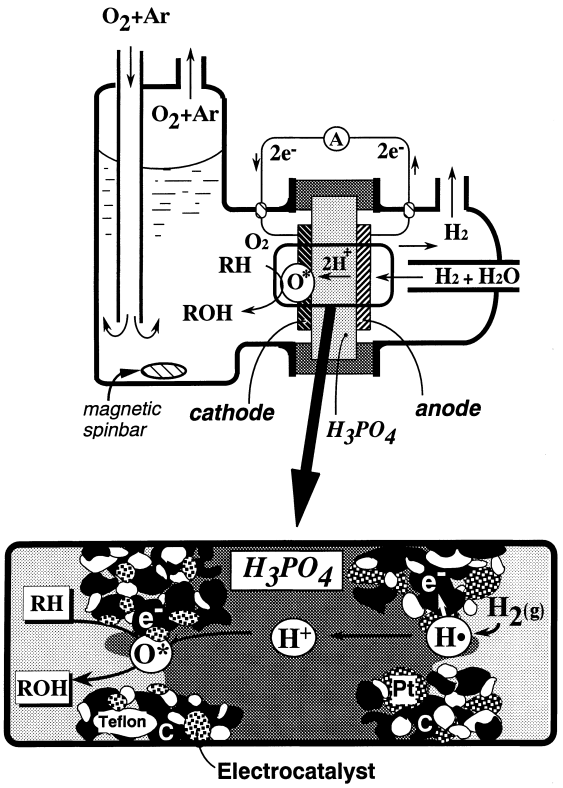

Fig. 1. Diagram of the H_2–O_2 cell for the direct oxygenation of hydrocarbons.

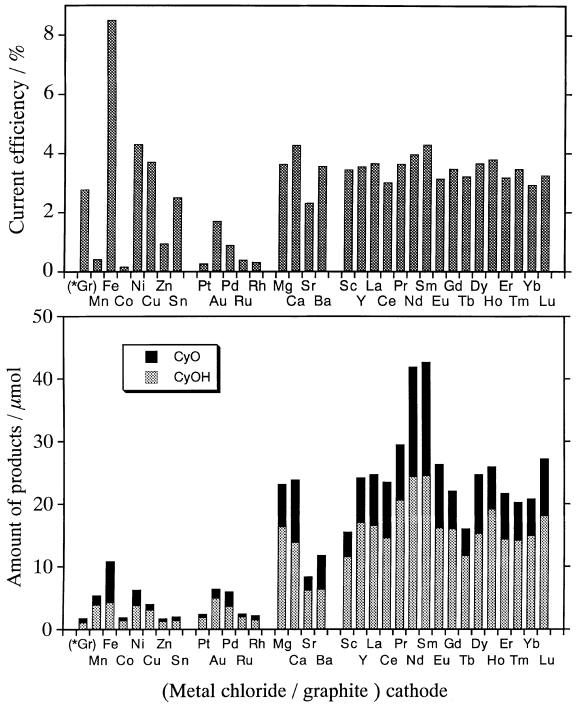

Fig. 2. Oxidation of cyclohexane over various cathodes during H_2–O_2 cell reactions. $T = 298$ K, reaction time = 20 h, superficial area of the cathode = 2.5 cm^2. Cell configuration: [O_2 (101 kPa), cyclohexane (40 ml) | cathode | H_3PO_4 aq. (1 mol l^{-1}) in silica–wool disk | anode | H_2 (98 kPa), H_2O (3.3 kPa)]. Cathode: metal chloride (0.5 mol%)/graphite (70 mg), anode: Pt-black (20 mg)/graphite (50 mg). *Gr; graphite only.

the cathode, the formation of the boundary is essential for the oxygenation of hydrocarbons.

The oxidation of hydrocarbons using the system in Fig. 1 was usually operated by batch type procedure. A potentiostat, an electrometer, a zero-shunt ammeter, and a reference electrode (Ag | AgCl) were used for electrochemical measurement. Products were analyzed by GC and HPLC. Details for the experiments have been reported elsewhere [23].

The cathodes were prepared from the electrocatalysts/graphite and PTFE powder by the hot-press method [23–25]. The graphite powder was used as a support for the electrocatalysts because of its superior electric conductivity, high chemical stability and catalytic inability for the oxidation. The electrocatalyst was added to the graphite by a conventional impregnation method from the solutions of metal salts or complexes. When the electrocatalyst was not soluble in solvents, it was physically mixed with graphite.

Many electrocatalysts in the cathode were tested for oxygenation of cyclohexane under short circuit conditions at 30°C. The results are shown in Fig. 2 [13,21–25]. No products were obtained under open circuit conditions for the cathodes tested in Fig. 2. The cathode with rare-earth metal chlorides, especially with $NdCl_3$ and $SmCl_3$, were active for oxygenations of cyclohexane to cyclohexanol (CyOH) and cyclohexanone (CyO) [13,23]. Constant current (ca. 5 mA) and steady formations of CyOH and CyO continued for the $SmCl_3$/graphite cathode for 20 h. Turnover number for the formation of oxygenates per one Sm^{3+} exceeded 2. It was obvious that the oxidation of cyclohexane proceeded catalytically. Assuming that two electrons are necessary for the formation of each oxygenated molecule (Eqs. (3) and (4)), the current efficiency for the formation of oxygenates is defined by Eq. (7).

$$\text{Current efficiency} = \frac{\text{(Sum of CyOH and CyO (mol))} \times 2 \times 100\ (\%)}{\text{Charge passed (C)}/96500\ (\text{C mol}^{-1})} \quad (7)$$

The current efficiencies observed for most of the rare-earth metal cations were in the rage of 3–4%. Although the current efficiency was low, this was the first case demonstrating that rare earth cations were better catalysts than transition metals or precious metal cations for the oxygenation of alkanes under mild condition [13].

As can be seen in Fig. 2, $FeCl_3$/graphite showed an electrocatalytic activity for the oxidation of cyclohexane. The current efficiency obtained for the $FeCl_3$/graphite was about twice as high as that of $SmCl_3$/graphite, though the yield of oxygenates for the former was far less than the latter. Fe cations are known to be the most typical active centers in the monooxygenase or monooxygenase mimic systems [1–10]. Therefore, it is interesting to compare the electrocatalytic functions of the two cathodes, $SmCl_3$/graphite and $FeCl_3$/graphite.

2.1.2. Character of active oxygen species on $SmCl_3$/graphite and $FeCl_3$/graphite cathodes

In order to get information about the electrocatalysis of $SmCl_3$ and $FeCl_3$, the effects of cathode potential on the oxidation of cyclohexane were studied.

Fig. 3 shows the effects of cathode potential on the formation rates of products in the cyclohexane oxidation and on the selectivity to cyclohexanol over $SmCl_3$/graphite and $FeCl_3$/graphite [13,23–25]. Under short-circuit conditions, the potentials for both cathodes were −0.24 V (vs. Ag | AgCl). The formation rate of oxygenates (CyOH + CyO) increased when the cathode potential decreased. However, when the cathode potential decreased below −0.24 V, the formation rates of oxygenates decreased because H_2 started to evolve intensely at the cathode for both cathodes [23]. In the case of $SmCl_3$/graphite, the selectivity to CyOH was roughly constant at all the potentials examined. In contrast with the $SmCl_3$/graphite, the selectivity to CyOH for $FeCl_3$/graphite increased from 35% at −0.24 V to 100% at +0.10 V. The cathode potential of the $FeCl_3$/graphite during the oxidation in Fig. 3 were lower than the standard redox potential of Fe^{3+}/Fe^{2+} of 0.54 V (vs. Ag | AgCl). Therefore, most

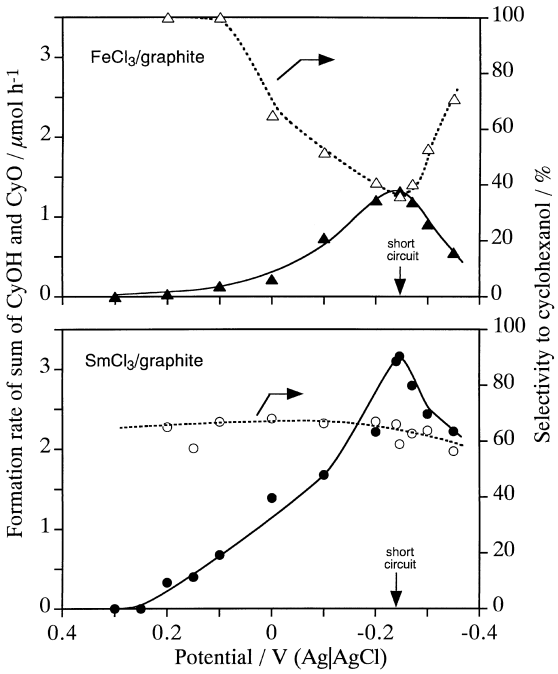

Fig. 3. Effects of the cathode potential on the partial oxidation of cyclohexane over $SmCl_3$/graphite and $FeCl_3$/graphite cathodes. $T = 298$ K, [O_2 (101 kPa), cyclohexane (40 ml) | cathode | H_3PO_4 aq. (1 mol l^{-1}) in silica–wool disk | anode | H_2 (98 kPa), H_2O (3.3 kPa)], reference electrode: Ag | AgCl, cathode: $SmCl_3$ or $FeCl_3$ (0.5 mol%)/graphite (70 mg), anode: Pt-black (20 mg)/graphite (50 mg).

of the iron cations must be in Fe^{2+} which would catalyse the reductive activation of O_2 and the oxygenation of cyclohexane [23–25]. Thus, the redox of Fe^{3+}/Fe^{2+} could be the driving force for the oxygenation of cyclohexane. In contrast with the iron cations, the redox of Sm^{3+}/Sm^{2+} cannot be expected under the reaction conditions in Fig. 3 because of a large negative redox potential ($Sm^{3+}/Sm^{2+} \approx -1.7$ V vs. Ag | AgCl). Therefore, the reaction mechanisms or the active oxygen species for the two cathodes must be quite different.

The reactivities of different hydrocarbons (hexane, adamantane, benzene, etc.) and their product distributions were compared between the two cathodes. Furthermore, kinetic isotope effects on the oxidation of cyclohexane, and the effect of a radical trap agent (CCl_4) on the cyclohexane oxidation were studied to get information about the reaction mechanism [23]. These results are summarized in Table 1.

Table 1
Reactivities of active oxygen species

Cathode	Regioselectivity $1^\circ:2^\circ:3^\circ$	Cyclohexane oxidation	
		k_H/k_D[a]	CCl_4 addition[b]
$SmCl_3$/graphite	1 : 4 : 10	1.7	0.96
$FeCl_3$/graphite	1 : 5 : 15	1.3	0.34

[a] Kinetic isotope effect evaluated on the basis of the amount of oxygenates from the oxidation of a mixture of cy-C_6H_{12} and cy-C_6D_{12} (1 : 1).
[b] The ratio of the product yields obtained with and without addition of CCl_4.

The regioselectivities of the active oxygen species to the primary (1°), secondary (2°), and tertiary (3°) C–H bonds oxygenated products per number of C–H bonds were evaluated from the relative amounts of products oxygenated at the corresponding carbons in *n*-hexane and adamantane oxidations. The regioselectivity ($1^\circ:2^\circ:3^\circ$) were 1 : 4 : 10 for $SmCl_3$/graphite and 1 : 5 : 15 for $FeCl_3$/graphite. The typical regioselectivity observed for $HO^\bullet$ and Fe–porphyrin were 1 : 5 : 15 and 1 : 25 : 250, respectively [1–4,26–28]. The regioselectivities observed for the two cathodes were close to that of $HO^\bullet$ but far from that of Fe–porphyrin. This suggests that the reactivities of active oxygen species on the two cathode are similar to that of $HO^\bullet$ in alkane oxidation.

The kinetic isotope effects (k_H/k_D) evaluated from the amounts of oxygenates in the oxidation of a mixture of cy-C_6H_{12} and cy-C_6D_{12} were 1.7 and 1.3 for the $SmCl_3$/graphite and $FeCl_3$/graphite, respectively. The small isotope effect observed for the $FeCl_3$/garphite has often been reported in the oxidations caused by $HO^\bullet$ ($k_H/k_D = 1.1$–1.3) [26–28].

The influence of addition of CCl_4 (a radical trapping agent) on the oxygenate yield in the cyclohexane oxidation was not observed for the $SmCl_3$/graphite but a large inhibition effect appeared for the $FeCl_3$/graphite. These results suggest that the active oxygen species on the $FeCl_3$/graphite has a radical character, but that on $SmCl_3$/graphite has not such character.

On the bases of the results in Table 1, we consider that the active species on $FeCl_3$/graphite is $HO^\bullet$ but that on $SmCl_3$ is different from $HO^\bullet$. Studies of cyclic voltammetry on the electrochemical reduction of O_2 on the $SmCl_3$/glassy carbon suggested that the active species was produced from an adduct of Sm^{3+} and hydrosuperoxide [23]. However, real form of active oxygen species has not been clarified yet.

2.1.3. ω-Oxidation with (FeCl$_3$ + cyclodextrin)/graphite cathode

In the case of oxidation of linear alkanes, selective oxygenation at the terminal carbons for the formation of primary alcohols and aldehydes is great significance because these compounds are used as the starting materials for the production of detergents and surfactants [11,29,30]. Among the metal chlorides tested as the cathode electrocatalysts for the oxidation of *n*-hexane during H_2–O_2 fuel cell reactions, $FeCl_3$ was the most active and stable electrocatalysts. Therefore, we have chosen the $FeCl_3$/graphite as the host cathode for the effect of cyclodextrin additives on the selective oxygenation at the primary carbons of *n*-hexane [30]. The selectivity to the primary-carbon oxygenated products (hexanal and 1-hexanol) was defined as the primary selectivity (PSel) [30] by Eq. (8).

$$\text{Primary selectivity (Psel)} = \frac{(\text{sum of hexanal and 1-hexanol})/6}{(\text{sum of 2- and 3-hexanols and 2- and 3- hexanones})/8} \quad (8)$$

Cyclodextrins are cyclic 1,4-linked D-glucopyranose oligomers comprising several glucose units and have the shape of hollow truncated cones. These cyclodextrins have very unique properties, i.e. hydrophilicity at the outer surface of cyclodextrins and hydrophobicity at the interior surface of their hollow structures (cavity). The cyclodextrins can accommodate many kinds of organic compounds with appropriate molecular dimensions in their hydrophobic cavities [31,32]. If *n*-hexane was introduced to the cavity of the cyclodextrin, methylene C–H bonds of *n*-hexane are to be blocked by the wall of the cyclodextrin from an attack of active oxygen species. Thus, we can expect that the oxygenation occurs exclusively at the terminal carbons.

Fig. 4 shows the effect of additions of α-, β-, γ-cyclodextrins(-CD) and glucose to the $FeCl_3$/graphite cathode on the product distribution and on the current for the oxidation of hexane by the same H_2–O_2 cell system as that in Fig. 1. The additions of cyclodextrins and glucose increased the current (charge passed). The enhancing effect of cyclodextrins and

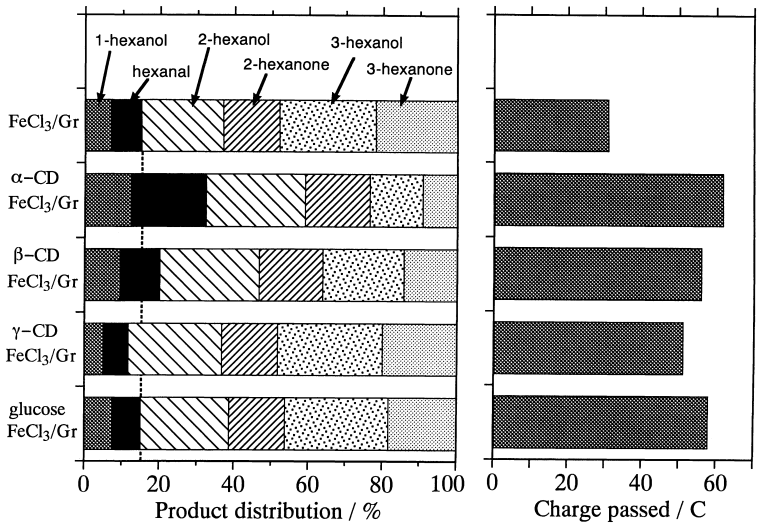

Fig. 4. Effects of addition of α-, β-, γ-cyclodextrins and glucose to the $FeCl_3$/graphite cathode on the ω-oxidation of *n*-hexane during H_2–O_2 cell reactions. $T = 298$ K, [O_2 (101 kPa), *n*-hexane (40 ml) | cathode | H_3PO_4 aq. (1 mol l^{-1}) in silica–wool disk | anode | H_2 (98 kPa), H_2O (3.3 kPa)], cathode: cyclodextrin or glucose (0.1 g) + $FeCl_3$ (0.5 mol%)/graphite (70 mg), anode: Pt-black (20 mg)/graphite (50 mg).

glucose on the current may be due to an increase in the area of the three-phase boundary, which increases the reaction zone of the electrochemical reduction of O_2. The total product yield of oxygenates increased according to the increase in the charge passed. When α- and β-cyclodextrin were added to the $FeCl_3$/graphite, the selectivity to the primary-carbon oxygenates was clearly increased compared with that of the normal $FeCl_3$/graphite cathode. The PSel for the (α-CD + $FeCl_3$) cathode was 0.63 and that for the (β-CD + $FeCl_3$) cathode was 0.33. However, γ-cyclodextrin and glucose did not increase the oxygenate at the primary carbon (PSel = 0.21). The increase in the PSel for the cathode modified by α- and β-cyclodextrins must be due to a good adaptation of *n*-hexane in the cavities of cyclodextrins.

The diameters of cavities of cyclodextrins are 0.47–0.53 (α-CD), 0.60–0.65 (β-CD), and 0.78–0.83 nm (γ-CD). The common depth of the cavities is about 0.79 nm. The molecular size of *n*-hexane is 0.49×0.82 nm. The hydrophobic nature of the interior of cyclodextrins can enhance the inclusion of *n*-hexane [32]. It seems that *n*-hexane molecule is just fitted to the diameter of the cavity of α-cyclodextrin but the molecule in the cavities of β- and γ-cyclodextrins may leave a large free space in the cavities. On the basis of the thermodynamic data concerning inclusion compounds of α- and β-cyclodextrin derivatives with *n*-hexane, Lammers has suggested the formation of 1 : 1 inclusion compounds [32]. He suggested that α-cyclodextrin derivatives include one *n*-hexane molecule in its stretched conformation in the interior of the cavity, whereas β-cyclodextrin derivatives would include the molecule in a compact coil form (but only loosely). The terminal carbons of *n*-hexane molecule in the α-cyclodextrin must protrude from the cavity. We suggest that the active oxygen generated during H_2–O_2 fuel cell reactions can attack only this primary carbon of *n*-hexane molecule included in the cavity of α-cyclodextrin. Although the PSel value of 0.63 observed for (α-CD + $FeCl_3$)/graphite is not so high as to be called ω-oxidation at the moment, the application of cyclodextrins or other host molecules capable for including *n*-alkanes could be a useful technique to realize the ω-oxidation of linear alkanes.

2.2. Hydroxylation of aromatics

2.2.1. Hydroxylation of benzene over various carbon cathodes

The cathodes of $SmCl_3$/graphite and $FeCl_3$/graphite described in the previous section were also effective for the hydroxylation of benzene to phenol during the H_2–O_2 cell reaction. However, the formation rates of

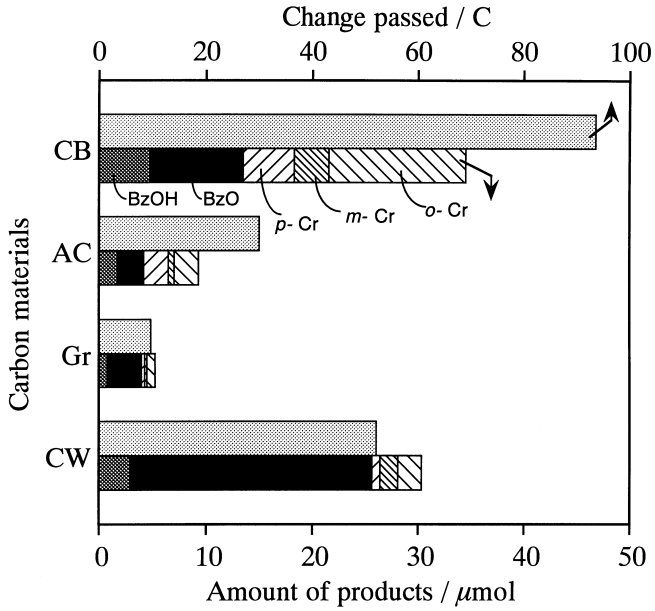

Fig. 5. Distribution of products in the oxidation of toluene on the cathodes prepared from different carbon materials during H_2–O_2 cell reactions. $T = 298$ K, [O_2 (101 kPa), toluene (40 ml) | cathode | H_3PO_4 aq. (1 mol l^{-1}) in silica–wool disk | anode | H_2 (98 kPa), H_2O (3.3 kPa)], cathode: carbon materials (70 mg) treated with hot HNO_3 aq., anode: Pt-black (20 mg)/graphite (50 mg). CB; carbon black, AC; active carbon, Gr; graphite, CW; carbon whisker.

oxygenates in the benzene oxidation as well as in the oxidation of cyclohexane should be enhanced as much as possible. So far, graphite powder (Gr) has been used as a support for the electrocatalysts in the cathode. However, the low surface area of graphite powder ($<2\,m^2\,g^{-1}$) cannot yield a large three-phase boundary in the cathode. As described in the introduction, the electrochemical reduction of O_2 must proceed at the three-phase boundary in the cathode. Thus, we tested first various carbon materials having high surface area as the cathode without additives to enhance the yield of oxygenates.

The carbon materials tested were carbon-whisker (CW, $22\,m^2\,g^{-1}$), carbon black (CB, $100\,m^2\,g^{-1}$), and active carbon (AC, $800\,m^2\,g^{-1}$). We found that those carbon materials pre-treated with a hot aqueous solution of HNO_3 became active for the hydroxylation of benzene to phenol (PhOH) without any additives [33]. The CW was the most active cathode among the HNO_3-treated carbon materials for the hydroxylation of benzene to PhOH (30 μmol in 3 h). The relative electrocatalytic activities were CW ≫ AC > CB ≫ Gr. The HNO_3-treatment causes the oxidation of the surface of carbon materials, forming functional groups such as carboxyl and quinone–hydroquinone groups. This would increase the hydrophilicity of the carbon surface, consequently increases the three-phase boundary in the cathode. Moreover, these functional groups could work as the catalytic sites for the reductive activation of O_2 even in the absence of metal cations.

2.2.2. Synergism of carbon materials on hydroxylation of toluene

The oxidation of toluene, instead of benzene, with the cathode of carbon materials described above gave *o*-, *m*-, *p*-cresols (the sum defined as CrOH), benzaldehyde and benzyl alcohol (the sum defined as BzOx). The formation rates of products and product distributions were quite different among the carbon materials as indicated in Fig. 5. Higher yields of products were obtained for the CW and CB cathodes but the distribution of the products were very different between the two cathodes [34,35]. The CW cathode was suitable for the formation of BzOx, while the CB cathode was favorable for the formation of CrOH. The selec-

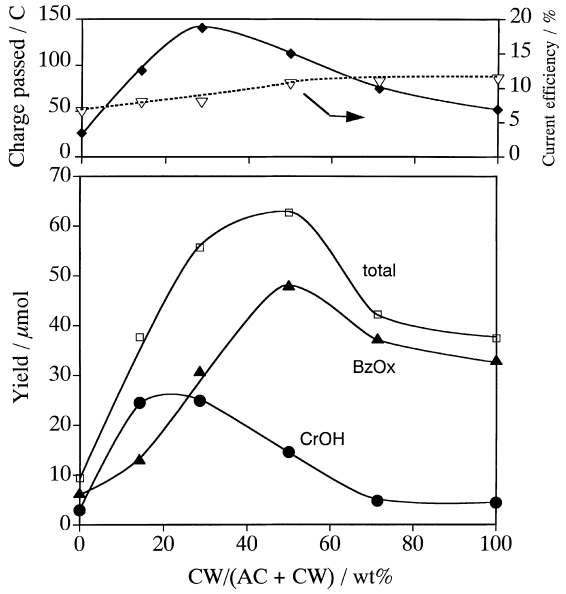

Fig. 6. Synergism of carbon whisker (CW) and active carbon (AC) on the oxidation of toluene during H_2–O_2 cell reactions. $T = 298$ K, [O_2 (101 kPa), toluene (40 ml) | cathode | H_3PO_4 aq. (1 mol l^{-1}) in silica–wool disk | anode | H_2 (98 kPa), H_2O (3.3 kPa)], cathode: CW + AC (70 mg), anode: Pt-black (20 mg)/graphite (50 mg). CrOH: sum of *o*-, *m*-, *p*-cresols, BzOx: sum of benzaldehyde and benzyl alcohol.

tivity to BzOx was high for the Gr cathode and that to CrOH was relatively high for the AC cathode, though the catalytic activities of the Gr and AC cathodes were low compared to those of CW and CB. We speculate that these differences in the catalytic activities as well as the product distributions can be ascribed to the differences in the kinds and the concentration of the catalytic functional groups on the surface of the carbon materials.

The cathodes prepared from the physical mixtures of CW and AC showed a synergism of the two carbon materials for the oxidation of toluene. Fig. 6 shows the yield of oxygenates for the toluene oxidation as a function of the weight percent of CW in the (CW + AC) cathode. When a small amount of CW was added to the AC cathode, the total yield of oxygenates was remarkably increased. The maximum yield of the sum of products was obtained for the cathode prepared from AC and CW by equal weight percent. The yield at the maximum was 6.5 and 1.6 times greater than those of the AC and CW cathodes, respectively. Product distribution changed remarkably with the weight percent of CW in the (CW + AC) cathode. The maximum selectivity to CrOH (65%) was obtained for the (CW(15 wt.%) + AC) cathode. In contrast, the maximum selectivity to BzOx (88%) was obtained for the (CW(70 wt.%) + AC) cathode. The strong synergism of physical mixture of CW and AC were observed both for the catalytic activity and the selectivity.

Similar synergism was observed for the cathode prepared from the mixture of $FeCl_3$/AC and CW. Toluene was selectively oxidized to CrOH with 90% selectivity for the $FeCl_3$/AC cathode without CW, though the catalytic activity was low. The CW cathode was a suitable cathode for the selective synthesis of BzOx as described above. The cathode prepared from a physical mixture of $FeCl_3$/AC and CW (5 : 2) increased the catalytic activity by five times of that of the $FeCl_3$/AC cathode, keeping a high selectivity to CrOH (93%) [32].

We speculate that the combination of different functional groups (such as hydroxyl-, hydroquinone-, quinone-, carboxyl-groups, etc.) on the surface of AC and CW could modify the electrocatalytic activity as well as the product selectivities for the oxidation of toluene on (AC + CW) cathodes, which may explain the synergism described above. The model for the synergism is based on the following three assumptions: (i) The active oxygen species generated on the carbon cathodes is $HO^{\bullet}$, (ii) oxidation of toluene takes place according to Fenton mechanism, (iii) CW and AC have different functional groups which catalyze the oxidation.

Major reaction paths in Fenton mechanism [23–28,38] for the oxidation of toluene are shown in Fig. 7. $HO^{\bullet}$ attacks to the phenyl ring of toluene, producing an *o*- or *p*-hydroxyl-hexadienyl-radical (A) intermediate. The intermediate (A) is oxidized to *o*- or *p*-CrOH by an oxidant through the path r2. The intermediate (A) can be converted to benzyl radical intermediate by dehydration and deprotonation through r3 and r4. This benzyl radical intermediate is oxidized with O_2 to benzaldehyde (BzO) and benzyl alcohol (BzOH). The product distributions were determined by relative reaction rates of r2 and (r3, r4, r5). In a typical Fenton system, the oxidant working at r2 is Fe^{3+} [26,27,36].

In the case of the CW cathode, it should be recalled that the major products were BzOx. On

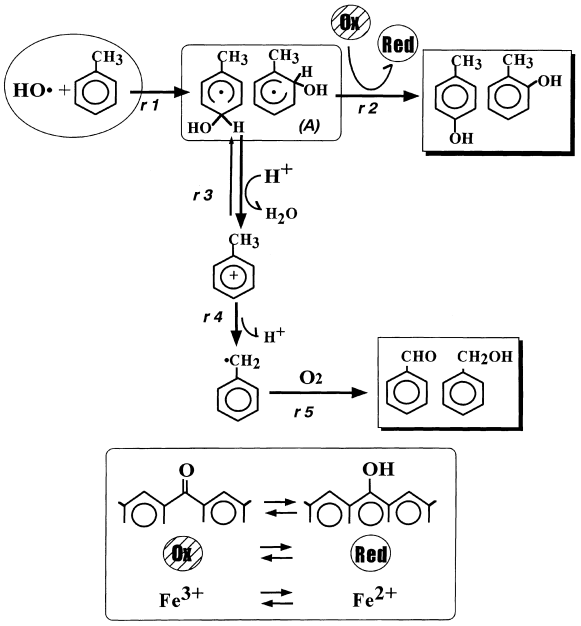

Fig. 7. Reaction scheme of Fenton mechanism for the oxidation of toluene.

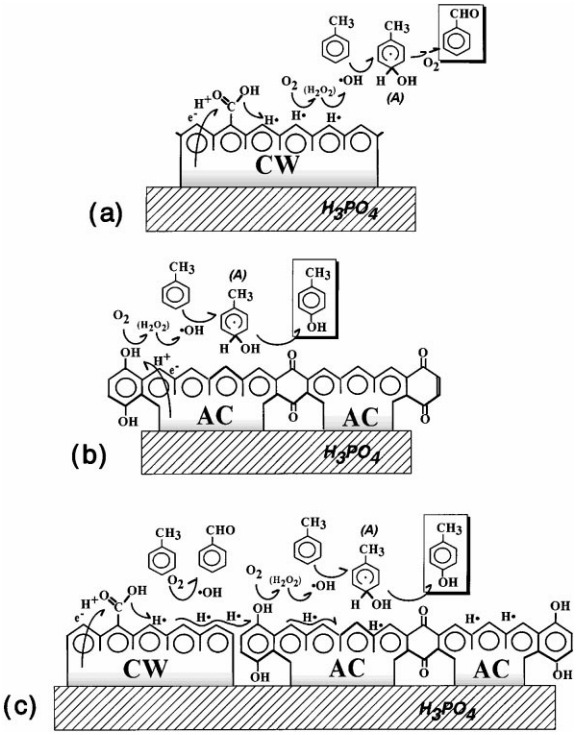

Fig. 8. Model of the reaction mechanism for the oxidation of toluene on CW (a), AC (b), and (CW + AC) (c) cathodes.

the basis of Fenton mechanism, BzOx are produced through the paths of r1, r3, r4, and r5, and the reaction rate of r2 must be slow, which suggests an oxidant for the formation of CrOH is absent on the CW cathode. We speculate that hydrogen species ($H^{\bullet}$) produced by the reduction of H^+ at the protonic functional groups (probably carboxyl-groups), reductively activate O_2 to $HO^{\bullet}$, as shown in Fig. 8a. This $HO^{\bullet}$ attacks to toluene producing the intermediate (A) which coverts mostly to BzOx as the major products.

In the case of the AC cathode, the major products were cresols (CrOH). This fact suggests the presence of an oxidant on the AC cathode enhancing the rate of r2. We believe that such oxidant could be a quinone group which works as a redox mediator (quinone/hydroquinone). The hydroquinone group reductively activates O_2 producing $HO^{\bullet}$, as shown in Fig. 8b. $HO^{\bullet}$ adds to toluene producing the intermediate (A) which coverts to CrOH as the major products due to the oxidation by the quinone-group (oxidant) on r2.

Fig. 8c shows a model of the synergism of CW and AC on the oxidation of toluene. We speculate that hydrogen species ($H^{\bullet}$) generated on the surface of CW migrates to the surface of AC. This hydrogen species reduces quinone-groups to hydroquinone groups which can reductively activate O_2 on AC. Thus, the formation rate of $HO^{\bullet}$ on AC is enhanced by the addition of CW to AC. When the weight percent of CW was <30%, the intermediate (A) is efficiently oxidized to CrOH by the quinone-groups remained on the surface of AC. When the weight percent of CW becomes >50%, the steady state concentration of quinone-groups would be decreased due to the reduction to hydroquinone-groups with the spillover hydrogen species from the surface of CW. Under these circumstances, the intermediate (A) is mainly converted to BzOx through r3, r4, and r5 in Fig. 7 because of the absence of quinone-group (oxidant at r2).

As described above, the synergism of CW and AC on the oxidation of toluene can be explained in terms of the spillover of active hydrogen from CW to AC and the redox catalyses of the surface functional groups (quinone/hydroquinone) on AC. We consider that H_2O_2 should be produced as a precursor for

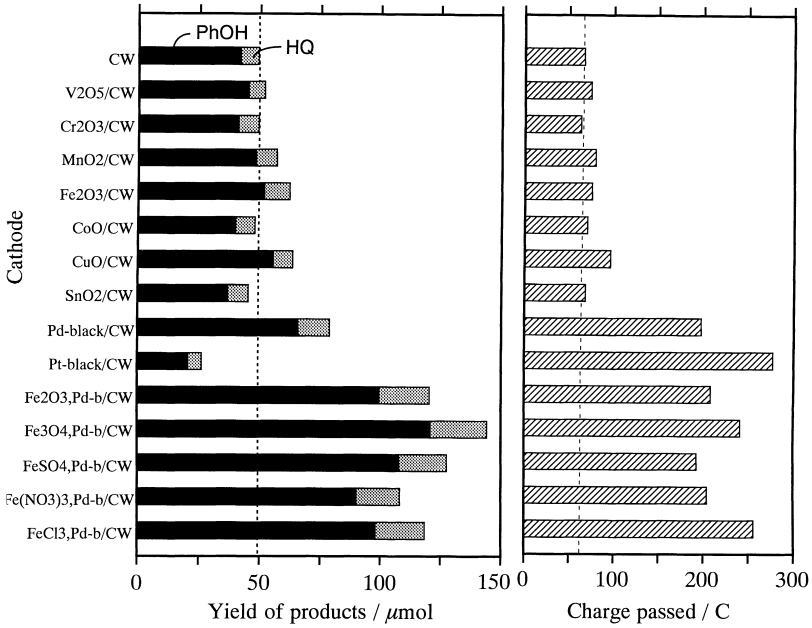

Fig. 9. Hydroxylation of benzene to phenol and hydroquinone over various cathodes based on carbon whisker (CW) during H_2–O_2 cell reactions. $T = 298$ K, reaction time = 3 h, short circuit conditions. Cell configuration: [O_2 (101 kPa), benzene (40 ml) | cathode | H_3PO_4 aq. (1 mol l^{-1}) in silica–wool disk | anode | H_2 (98 kPa), H_2O (3.3 kPa)]. Cathode: metal oxide (5 mg) and/or precious metal (20 mg)/carbon whisker (50 mg). Anode: Pt-black (20 mg)/graphite (50 mg).

$HO^{\bullet}$ over the cathode. We examined the formation of H_2O_2 in H_3PO_4 aqueous solution in the membrane during the oxidation. No accumulation of H_2O_2 was observed in the aqueous phase. If H_2O_2 was produced on the cathode during the cell reactions, H_2O_2 should immediately reduce to $HO^{\bullet}$ or H_2O under reaction conditions.

2.2.3. Effects of additives in CW cathode on the hydroxylation of benzene

In order to improve the catalytic activity of the CW cathode for the hydroxylation of benzene, the favorable effects of the addition of various metal compounds to the cathode were examined [33,37]. Fig. 9 shows the yields of PhOH and hydroquinone (HQ) obtained for the CW cathodes with various additives. Compared with the results of CW alone (uppermost), the addition of Pd-black to CW (Pd-black/CW) increased the current and the yields of PhOH and HQ. When Pt-black was added to the CW cathode, the current increased by four times of that of CW cathode, but the yield of oxygenates decreased to about a half of that of CW. In the case of Fe_2O_3/CW cathode, the total yield of PhOH and HQ increased by ca. 1.3 times of that of the CW cathode, but the increase in the charge passed was only a slight. Therefore, the addition of Fe_2O_3 improved the current efficiency for the formation of PhOH and HQ. Co-addition of Pd-black and Fe_2O_3 to CW remarkably accelerated the formation of PhOH and HQ, suggesting a synergism of the two compounds. Other combinations between each of the electrocatalysts in (Pd, Pt, Rh, Ru and the oxides of Fe, Cu, Mn, Co, Sm, and La) did not accelerate the formations of PhOH and HQ, except for the combination of Pd-black and Fe-compounds ($FeCl_3$, Fe_3O_4, $Fe(NO_3)_3$, $FeCl_2$, $FeSO_4$). Among these Fe-compounds, Fe_3O_4 was the most effective electrocatalyst for the formation of phenols in the presence of Pd-black as can be seen in Fig. 9. These results strongly indicate the synergism of Pd-black and Fe-compounds on the hydroxylation of benzene to PhOH and HQ.

We propose here a tentative reaction mechanism on the basis of our experimental results, as below. The active oxygen species over the CW cathodes both in

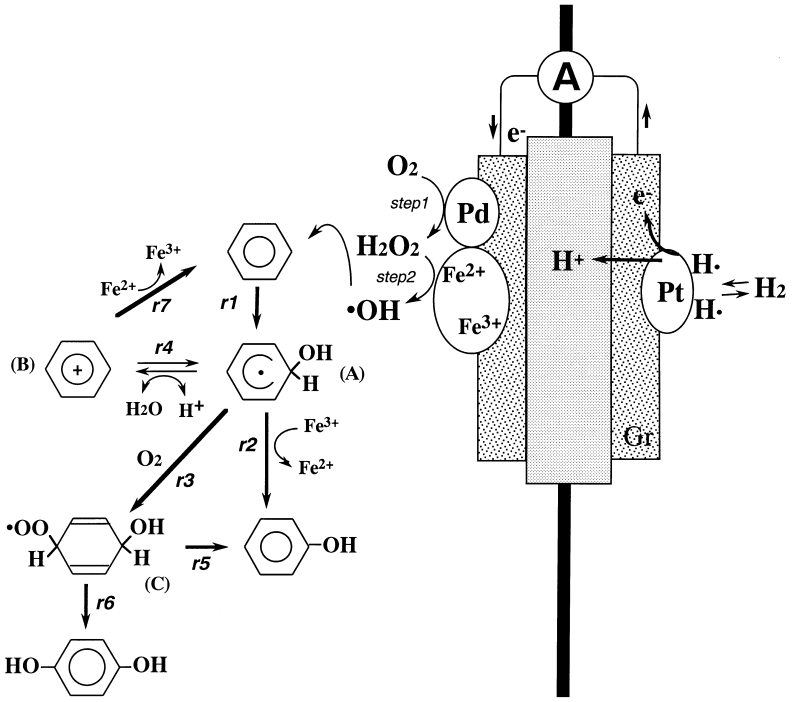

Fig. 10. Reaction mechanism for the synergism of Pd-black and Fe_3O_4 and the hydroxylation of benzene.

the absence and presence of additives of Pd-black and Fe_3O_4 must be $HO^{\bullet}$ radical [13,21–28,33–37]. In this case, the hydroxylation of benzene proceeds through the Fenton Chemistry as already been discussed in Fig. 7. The synergism of Pd-black and Fe_2O_3 can be explained in terms of the cooperative actions of the additives, which is demonstrated schematically in Fig. 10. It is reasonable to assume that Pd^0 accelerates the reduction of O_2 into H_2O_2 (step 1) during the H_2–O_2 cell reaction [21]. The acceleration in the reduction of O_2 increases the current or the charge passed which was actually observed in Fig. 9. The redox of Fe^{3+}/Fe^{2+} on Fe_3O_4 enhances the generation of $HO^{\bullet}$ from H_2O_2 (step 2) according to the following equation:

$$H_2O_2 + Fe^{2+} + H^+ \rightarrow HO^{\bullet} + Fe^{3+} + H_2O \qquad (9)$$

This $HO^{\bullet}$ attacks benzene producing PhOH and HQ as demonstrated in the Fenton Chemistry [23–28,33–36]. The addition of $HO^{\bullet}$ to benzene produces a hydroxyl-hexadienyl-radical (A) intermediate. The intermediate (A) is oxidized to PhOH by Fe^{3+} (r2). If the intermediate (A) is oxidized with O_2 (r3), PhOH is also produced via r5 and HQ via r6. The intermediate (A) could be dehydrated into phenyl cation intermediate (B) by acid catalysis (r4). This intermediate (B) may be reduced back to benzene by a reductant such as Fe^{2+} or H–Pd (r7).

The synergism of Pd-black and Fe-compounds on the hydroxylation of benzene was explained by the following three enhancing effects. These are (i) the increase in the rate of formation of H_2O_2 due to the electrocatalytic function of Pd-black (step 1), (ii) the acceleration in the generation of $HO^{\bullet}$ according to Eq. (9) through the redox of Fe^{3+}/Fe^{2+} of the Fe-compounds (step 2), and (iii) the enhancement of the rate of oxidation of intermediate (A) by Fe^{3+} (at r2) [36,37].

We speculated the formation of H_2O_2 on the (Pd-black + Fe-compound)/CW cathode during the cell reactions but no accumulation of H_2O_2 was observed in the membrane after the oxidation. If H_2O_2 was produced on the cathode, it must be immediately reduced to $HO^{\bullet}$ and H_2O under the reaction conditions. The effect of the addition of H_2O_2 aq. to the aqueous membrane on the hydroxylation of ben-

zene was studied. The formation of phenol was not observed under open circuit conditions. Under short circuit conditions, phenol was certainly produced during H_2O_2–H_2 cell reactions but the yield of phenol was lower than 1/5 times of that during O_2–H_2 cell reactions. These results suggest that in situ synthesis of H_2O_2 on the cathode is essential to generate active oxygen species for the hydroxylation.

2.2.4. Cogeneration of oxygenates and electricity

The hydroxylation of benzene on the (Pd-black + Fe-compounds)/CW cathode described so far has been carried out under short circuit conditions. The cathode potential of this electrode under short-circuit conditions (−0.22 V vs. Ag | AgCl) did not change appreciably with the change in the conditions of the cathode (Pd-black/Fe-compounds ratios, partial pressures of O_2, concentration of benzene, etc.). It is interesting to examine the effect of the terminal voltage on the hydroxylation of benzene by changing the externally-applied voltage. The terminal voltage is the relative potential of the cathode with reference to the anode. The anode potential was almost constant (≈0 V vs. NHE) under the reaction conditions in Fig. 11. The yield of phenol and the charge passed for the (Pd-black + Fe_2O_3)/CW are plotted as functions of the terminal voltage in Fig. 11 (dotted curve). The results for this cathode indicate that the highest yield of phenol is obtained at the terminal voltage of −0.1 V. The negative terminal voltage <−0.1 V decreased the phenol formation, thus the current efficiency drastically decreased with negative terminal voltage. The results for the CW cathode without additives and for those with CuO, Fe_2O_3, SnO_2, Mn_2O_3 or Cr_2O_3 are also plotted in Fig. 11. Except for the CuO/CW cathode, the yield of phenol increased with a decrease in the terminal voltage from +0.2 to −0.3 V. The maximum phenol yield was obtained at the terminal voltage of −0.1 ∼ −0.5 V, which corresponded to the cathode potential of −0.32 ∼ −0.72 V vs. Ag | AgCl. On the other hand, the CW cathode added with CuO showed very specific effect of the terminal voltage on the formation rate of phenols as well as on the current. The current and the yield of phenol were accelerated with a rise in the terminal voltage from 0 to +0.30 V. The maxima in the current and the formation rate of phenol were obtained at a terminal voltage of ca. +0.30 V. Very similar effects of the terminal voltage were observed for the CW cathodes added with other copper compounds such as $CuSO_4$, $Cu(NO_3)_2$, $Cu(OAc)_2$, $CuCl_2$, and CuCl. The most effective Cu-compound for the formation of phenol was $CuSO_4$ [21]. For this cathode, the maximum current was obtained at a cell voltage between +0.20 and +0.30 V. The electric power output shows the maximum (1.5 mW cm^{-2}) at a cell voltage of +0.20 ∼ +0.30 V. The amount of the sum of PhOH and HQ gave the maximum at +0.30 V.

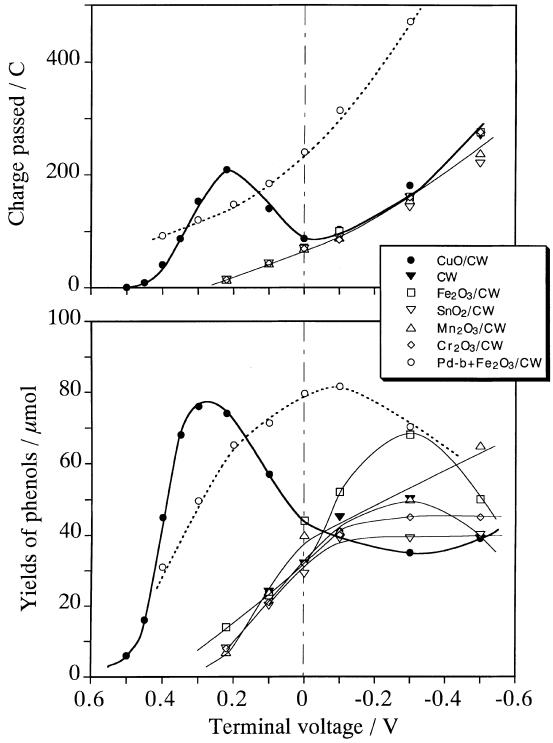

Fig. 11. Effect of the terminal voltage on the hydroxylation of benzene for various cathodes based on carbon whisker. Terminal voltages; +0.5 ∼ −0.5 V, reaction time; 2 h, cathode; metal oxide (5 mg)/CW (70 mg). Other conditions were the same as Fig. 9.

The cathode potential for the $CuSO_4$/CW under short circuit conditions was −0.21 V (vs. Ag | AgCl). The potential at a terminal voltage of +0.30 V was +0.06 V (vs. Ag | AgCl). The redox potentials of copper are −0.044 V (Cu^{2+}/Cu^{+} vs. Ag | AgCl), +0.140 V (Cu^{2+}/Cu^{0}), and +0.324 V(Cu^{+}/Cu^{0}). Considering these potentials, we can expect the formations of H_2O_2 and $HO^{\bullet}$ through Eqs. (10) and (11) [38,39].

$$O_2 + 2Cu^{+} + 2H^{+} \rightarrow H_2O_2 + 2Cu^{2+} \quad (10)$$

$$H_2O_2 + H^+ + Cu^+ \rightarrow OH^\bullet + H_2O + Cu^{2+} \quad (11)$$

$$C_6H_6 + HO^\bullet + Cu^{2+} \rightarrow C_6H_5OH + Cu^+ + H^+ \quad (12)$$

The $HO^\bullet$ attacks benzene, forming PhOH in Eq. (12). The formation of PhOH proceeds through the similar mechanism to that of Fenton chemistry by replacing the redox of Fe^{3+}/Fe^{2+} to that of Cu^{2+}/Cu^+ [38,39]. Therefore, the redox of Cu^{2+}/Cu^+ on CW controls the rate of reduction of O_2 (current) and the yield of PhOH. When the terminal voltage decreases from +0.50 to +0.30 V, the reduction rate of Cu^{2+} to Cu^+ must be accelerated, increasing the current as well as the formation rate of PhOH as can be seen in Fig. 11. When the terminal voltage decreases further from +0.30 to 0 V (short circuit conditions), the cathode potential decreases to $-0.06 \sim -0.21$ V (Ag | AgCl) which inevitably converts Cu^{2+} and Cu^+ into Cu^0. Therefore, the steady state concentration of copper cations decreases, which should reduce the current and the formation rate of $HO^\bullet$, consequently the yield of phenols.

The H_2–O_2 fuel cell system described above can cogenerate oxygenates and electricity if we put a load in the outer circuit (chemical cogeneration). However, for every chemical cogeneration systems reported so far [17–21], the generation of electric power output by putting load in the outer circuit always reduced the production of chemicals because of the decrease in the current compared to the results at the short-circuit conditions. Under these circumstances, the copper compound-added cathodes are very specific in the sense that both the maximum electric power output and the maximum production of phenols can be obtained at the same terminal voltage.

2.3. Oxidation of light alkanes

2.3.1. Oxygenation in the gas phase

Partial oxidation of light alkanes such as CH_4, C_2H_6, and C_3H_8 into their alcohols and aldehydes is one of the most attractive subjects for the utilization of natural gas as a chemical feed stock. Therefore, we applied the same H_2–O_2 cell reactor described above for the oxidation of light alkanes by bubbling them into solvent such as CH_2Cl_2. However, the oxidations of CH_4, C_2H_6, and C_3H_8 were not successful by applying the same cathodes used for the hydroxylation of benzene such as (Pd-black + Fe_3O_4)/CW, $CuSO_4$/CW and $SmCl_3$/graphite. This might be due to a low solubility of light alkanes in the solvents compared with the oxidation of benzene and cyclohexane. Therefore, the light alkanes (g) were directly supplied to the cathode of the H_2–O_2 cell without using any solvent [40]. In other words, a gas mixture of light alkanes and O_2 was passed through the cathode compartment and hydrogen and water vapor flowed in the anode one. Both compartments were separated by a silica–wool disk containing aqueous H_3PO_4 (1 M). The screening of carbon materials suitable for the partial oxidation of propane concluded that the cathodes made from the carbon whisker (CW) [41] and the vapor phase-grown-carbon-fiber (VGCF) [42] were active for the oxidation of light alkanes at room temperature even in the absence of additives in the cathodes. Both carbon materials have no micropores and showed good electric conductivity and high chemical stability.

The effect of various electrocatalysts on the oxidation of propane was examined by using the VGCF as the host carbon material of the cathode. Fig. 12 shows the effects of the addition of Pd-black and vanadyl acetylacetonate ($VO(acac)_2$) on the oxidation of propane in the gas phase during the H_2–O_2 cell reaction. The products were acetone, acetic acid, and CO_2. When a mixture of propane and O_2 was passed through the cathode compartment under open circuit conditions, no products were observed. The comparison of the results in Fig. 12 suggests the synergism of $VO(acac)_2$ and Pd-black on the oxidation of propane. The addition of Pd-black to VGCF increased the current more than five times but the yield of products decreased drastically. When $VO(acac)_2$ was added to the VGCF cathode, the formation rates of products decreased clearly, indicating that $VO(acac)_2$ itself cannot enhance the catalysis of the VGCF cathode. However, co-addition of $VO(acac)_2$ and Pd-black considerably enhanced the activity of the propane oxidation. The selectivities to acetone and acetic acid on the basis of the propane reacted were 48 and 12%, respectively.

2.3.2. Propane oxidation over $(VO(acac)_2$ + Pd-black)/VGCF cathode

Fig. 13 shows the effects of partial pressure of propane on the formation rates of acetone, acetic acid, and CO_2 for the ($VO(acac)_2$ + Pd-black)/VGCF

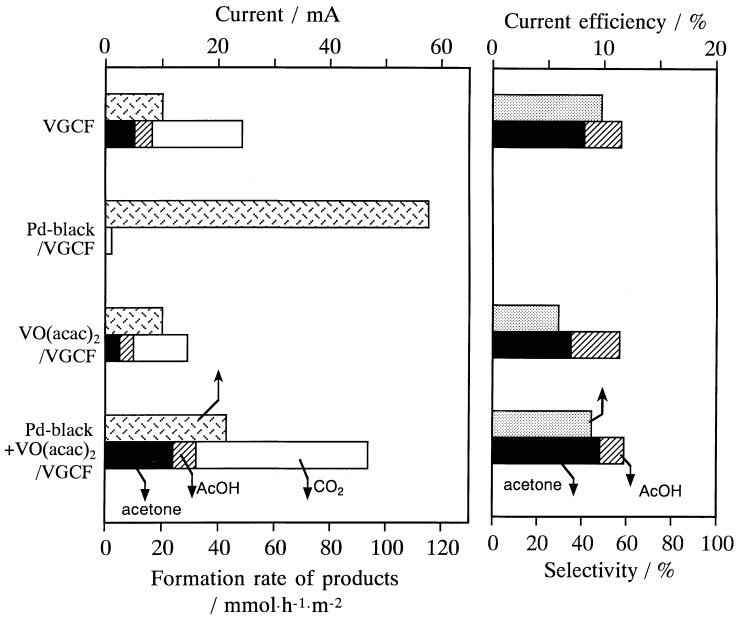

Fig. 12. Oxidation of propane in the gas phase with the cathodes based on VGCF during H_2–O_2 cell reactions. $T = 298$ K, specific area of the electrodes 2 cm^{-2}. Cell configuration: [O_2 (50.5 kPa), propane (50.5 kPa), cathode | H_3PO_4 aq. (1 mol l^{-1}) in silica–wool disk | anode, H_2 (48.5 kPa), H_2O (4 kPa)]. Total flow rate was 10 ml min^{-1}. Cathode: Pd-black (0.5 mol%) + $VO(acac)_2$ (1 mol%) + VGCF (50 mg). Anode: Pt-black (20 mg) + Gr (50 mg).

cathode under a constant partial pressure of oxygen of 50 kPa in the cathode compartment. In the upper part of the figure, the current and the current efficiency of the sum of acetone and acetic acid are plotted. The current decreased with increasing $P(C_3H_8)$, which may be ascribed to the competitive adsorption of O_2 and C_3H_8 on the active site because the current is determined mainly by the rate of reduction of O_2. The formation rate of acetone increased sharply with increasing $P(C_3H_8)$ in contrast with the decrease in the current. The formation rate of acetone depended on $P(C_3H_8)$ by second order. The current efficiency for the oxidation products at high $P(C_3H_8)$ reached to 10%. This value was quite high compared to the ones observed in the oxidation of benzene or cyclohexane ($\leqslant$5%). These results suggest that a radical chain mechanism may govern the oxidation of propane and the formation of acetone. We speculate that the activation of propane is cause by a free $HO^\bullet$ evolved into the gas-phase at the vicinity of the interface of electrode/electrolyte. The CW and VGCF, which have high outer surface without micropores, may be suitable for releasing $HO^\bullet$ into the gas phase. It was suggested that the free $HO^\bullet$ was a stronger oxidant than hydrated one [28]. The oxidation of propane must proceed mainly via radical chain mechanism initiated by the free $HO^\bullet$ in the gas phase.

We propose here a tentative mechanism for the synergism of Pd-black and $VO(acac)_2$ on VGCF, as below. It is reasonable to consider that Pd^0 accelerates the reduction of O_2 into H_2O_2, as described for the (Pd-black + Fe_3O_4)/CW cathode. We hypothesize that the redox of V^{4+}/V^{3+} enhances the generation of $HO^\bullet$ from H_2O_2 according to the following equation:

$$H_2O_2 + V^{3+} + H^+ \rightarrow HO^\bullet + V^{4+} + H_2O \qquad (13)$$

This $HO^\bullet$ abstracts hydrogen from the C–H bond of propane generating $C_3H_7^\bullet$ in the gas phase. O_2 adds to $C_3H_7^\bullet$ producing $C_3H_7OO^\bullet$. This peroxide radical reacts with propane being converted into acetone, cogenerating H_2O and $C_3H_7^\bullet$. The $C_3H_7^\bullet$ contributes in the propagation of the radical chain reactions. Thus, the formation of acetone should depend on the second order of $P(C_3H_8)$, which was actually observed

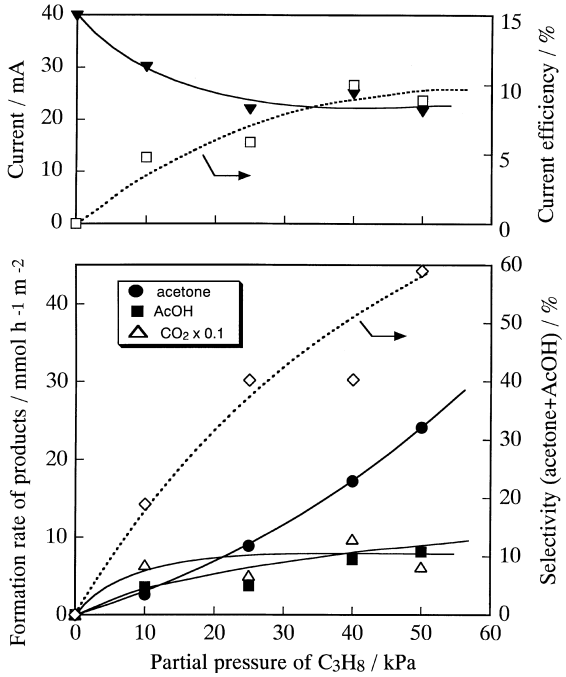

Fig. 13. Effect of $P(C_3H_8)$ on the oxidation of propane in the gas phase with (Pd-black, $VO(acac)_2$)/VGCF cathode during H_2–O_2 cell reactions. $P(C_3H_8) = 0 \sim 50.5$ kPa, $P(O_2) = 50.5$ kPa, other reaction conditions were the same as Fig. 12.

in Fig. 13. The synergism of Pd-black and $VO(acac)_2$ can be explained by the similar idea that has already been described in the case of (Pd-black + Fe_3O_4)/CW cathode in Fig. 10.

The ($VO(acac)_2$ + Pd-black)/VGCF cathode was applied also for the oxidations of CH_4 and C_2H_6 at 301 K. In the case of CH_4 oxidation, the product was only CO_2. Methanol, formaldehyde, and formic acid were not detected. However, it should be noted that CH_4 can be activated at room temperature, although the product is CO_2. In the case of C_2H_6 oxidation, CO_2 was also the main product but acetic acid was produced with 22% selectivity. In contrast with the results of CH_4 and C_2H_6, the oxidation of C_3H_8 produced the useful oxygenate (acetone and acetic acid) with relative high selectivity of 60%. The rate of alkane oxidation increased as CH_4 (current efficiency 0.5%) < C_2H_6 (5%) < C_3H_8 (10%), as we expected. This result suggests that the strength of C–H bond would determine the rate of oxidation. Further studies on the reaction mechanism and design of electrocatalysts are necessary to enhance the rate and the selectivity of oxygenates from the light alkanes.

3. Conclusion

As described so far, the reductively activated oxygen at the cathode of H_2–O_2 fuel cell realized the selective oxygenation of C6 alkanes and aromatics and non-selective oxidation of light alkanes at room temperature. However, we have not succeeded epoxidation of alkenes. The reason for this may be that the active oxygen species generated on most of the cathodes is $HO^{\bullet}$. It is well known that $HO^{\bullet}$ is active for the hydroxylation of aromatics and oxygenation of alkanes but not so for the epoxidation of alkenes [26–28]. In the case of $SmCl_3$/graphite cathode, the active oxygen species was suggested to be the one different from $HO^{\bullet}$ [23]. In fact, we confirmed that $SmCl_3$ catalyzed the epoxidation of alkenes with reductively activated oxygen by Zn and $MeCO_2H$ in the liquid phase [42,43]. This fact suggests a possibility that, if we can design a proper cathode with rare earth metal cations, the epoxidation of alkenes may be realized during the H_2–O_2 cell reactions.

The most serious problem to be solved for all the systems described in this review is to improve the current efficiency and the formation rate of oxygenates. Therefore, more active and selective electrocatalysts, more appropriate electrolytes, and better design for enhancing the three phase boundaries are definitely to be developed. At the moment, the method introduced in this work could be applied for the synthesis of expensive chemicals to compensate the low reaction rate and current efficiency.

As described above, the epoxidation of alkenes did not succeed with the H_2–O_2 cell system yet but the epoxidation of propene and hexene succeeded at the anode with Pt-black (PtO_2/Pt) and PtO_2/graphite during the electrolytic decomposition of H_2O at room temperature [44,45]. If benzene and O_2 are present in the cathode compartment by using (Pd-black + Fe_3O_4)/CW cathode, we can expect both cathodic hydroxylation of benzene and anodic epoxidation of alkenes at the same time [21,22,46]. These cogeneration of chemicals both at the cathode and the anode and the cogeneration of chemicals and electric-

ity described earlier may become attractive processes in the next century.

References

[1] J.T. Groves, T.E. Nemo, J. Am. Chem. Soc. 105 (1983) 5786.
[2] J.T. Groves, T.E. Nemo, J. Am. Chem. Soc. 105 (1983) 6243.
[3] P.R. Ortiz de Montellano, Cytochrome P-450, Structure, Mechanism and Biochemistry, Plenum, New York, 1986.
[4] F. Montanari, L. Casella, Metalloporpyrins Catalyzed Oxidations, Kluwer Academic, Netherlands, 1994.
[5] J. Green, H. Dalton, J. Biochem. 236 (1986) 155.
[6] L. Shu, J.C. Nesheim, K. Kauffmann, E. Münck, J.D. Lipscomb, L. Que Jr., Science 275 (1997) 515.
[7] I. Tabushi, N. Koga, J. Am. Chem. Soc. 101 (1979) 6456.
[8] D. Mansuy, M. Fontecave, J.F. Bartoli, J. Chem. Soc., Chem. Commun. (1983) 253.
[9] R. Battioni, J.F. Bartoli, P. Ledoc, M. Fontecave, D. Mansuy, J. Chem. Soc., Chem. Commun. (1987) 791.
[10] I. Tabushi, A. Yazaki, J. Am. Chem. Soc. 103 (1981) 17771.
[11] N. Herron, C.A. Tolman, J. Am. Chem. Soc. 109 (1987) 2837.
[12] A. Kunai, T. Wani, Y. Uehara, F. Iwasaki, Y. Kuroda, S. Ito, K. Sasaki, J. Chem. Soc. Jpn. 62 (1989) 2613.
[13] K. Otsuka, I. Yamanaka, K. Hosokawa, Nature (London), 345 (1990) 697.
[14] K. Otsuka, I. Yamanaka, K. Hosokawa, Chem. Lett. (1990) 509.
[15] T. Miyake, M. Hamada, Y. Sasaki, M. Oguri, Appl. Catal. A 131 (1995) 33.
[16] T. Hayashi, K. Tanaka, M. Haruta, J. Catal. 178 (1998) 566.
[17] S.H. Langer, S. Yurchak, J. Electrochem. Soc. 116 (1969) 1128.
[18] S.H. Langer, J.A. Colucci-Rios, Chem. Tech. (1985) 226.
[19] C.G. Vayenas, R.D. Farr, Science 208 (1980) 593.
[20] C.G. Vayenas, S.I. Bebelis, C.C. Kyriazis, Chem. Tech. 422 (1991).
[21] K. Otsuka, I. Yamanaka, Catal. Today 41 (1998) 311.
[22] K. Otsuka, I. Yamanaka, Hyoumen (Surface) 27 (1989) 473.
[23] I. Yamanaka, K. Otsuka, J. Chem. Soc., Faraday Trans. 89 (1993) 1791.
[24] I. Yamanaka, K. Otsuka, J. Chem. Soc., Faraday Trans. 90 (1994) 451.
[25] I. Yamanaka, K. Otsuka, J. Electrochem. Soc. 138 (1991) 1033.
[26] C. Walling, R.A. Jonson, J. Am. Chem. Soc. 97 (1973) 363.
[27] C. Walling, D.M. Camaiono, S.S. Kim, J. Am. Chem. Soc. 100 (1978) 4814.
[28] D.T. Sawyer, Oxygen Chemistry, Oxford University Press, New York, 1991.
[29] B.R. Cook, T.J. Reinert, K.S. Suslick, J. Am. Chem. Soc. 108 (1986) 7281.
[30] K. Otsuka, K. Furuya, Electrochem. Acta 37 (1992) 1135.
[31] J. Szeitli, Cyclodextrin Technology, Kluwer Academic, Dordrecht, 1988.
[32] J.N.J.J. Lammers, Recueil 91 (1972) 1163.
[33] K. Otsuka, M. Kunieda, H. Yamagata, J. Electrochem. Soc. 139 (1992) 2383.
[34] K. Otsuka, K. Ishizuka, I. Yamanaka, Chem. Lett. (1992) 773.
[35] K. Otsuka, K. Ishizuka, I. Yamanaka, Electrochim. Acta 37 (1992) 2549.
[36] T. Matsue, M. Fujihira, T. Osa, J. Electrochem. Soc. 128 (1981) 2565.
[37] K. Otsuka, M. Kunieda, I. Yamanaka, Stud. Surf. Sci. Catal. 82 (1994) 703.
[38] K. Sasaki, S. Ito, Y. Saheki, T. Kinoshita, T. Yamasaki, J. Harada, Chem. Lett. (1983) 37.
[39] S. Ito, T. Yamasaki, H. Okada, S. Okino, K. Sasaki, J. Chem. Soc. Perkin Trans. 2 (1988) 285.
[40] I. Yamanaka, T. Akimoto, K. Otsuka, Electrochem. Acta 39 (1994) 2545.
[41] Q. Zhang, K. Otsuka, Chem. Lett. (1997) 363.
[42] K. Otsuka, I. Yamanaka, Ye wang, Stud. Surf. Sci. Catal. 119 (1998) 15.
[43] I. Yamanaka, K. Otsuka, J. Mol. Catal. 83 (1993) L15.
[44] K. Otsuka, T. Ushiyama, I. Yamanaka, K. Ebitani, J. Catal. 157 (1995) 450.
[45] I. Yamanaka, K. Sato, K. Otsuka, Electrochem. Sol. St. Lett. 2 (1999) 131.
[46] K. Otsuka, I. Yamanaka, M. Hagiwara, Chem. Lett. (1994) 1861.